

Usefulness of liquid-crystal oral formulations to enhance the bioavailability and skin tissue targeting of *p*-amino benzoic acid as a model compound

Wesam R. Kadhum^a, Takeshi Oshizaka^a, Hijikuro Ichiro^b, Hiroaki Todo^a, Kenji Sugibayashi^{a,*}

^a Faculty of Pharmaceutical Sciences, Josai University, 1-1 Keyakidai, Sakado, Saitama 350-0295, Japan

^b Farnex Incorporated, Yokohama-shi, Kanagawa, Japan

* To whom correspondence should be addressed:

Kenji Sugibayashi, Ph.D.

Faculty of Pharmaceutical Sciences, Josai University

1-1 Keyakidai, Sakado, Saitama 350-0295, Japan

Tel.: 049-271-7367

Fax: 049-271-8137

E-mail: sugib@josai.ac.jp

Abstract

Topical formulations are not always suitable to deliver active ingredients to large areas of skin. Thus, in this study, we aimed to develop an oral formulation for skin tissue targeting with a high bioavailability using liquid crystals (LCs) dispersions comprising cubosomes of a mal-absorptive model compound, *p*-amino benzoic acid (PABA), which is an active element in cosmeceuticals, dietary supplements and skin disorder medicines. The bioavailability and skin concentration of PABA were investigated after oral administration in rats. The effect of the remaining amount of the LCs formulation in the stomach on the pharmacokinetic profiles of orally administered PABA was evaluated. The skin permeation and concentration of PABA were also investigated using an *in vitro* permeation experiment. As a result, the bioavailability of PABA was significantly improved by administration of PABA-LC formulations compared with PABA solution alone, although the effect was greatly influenced by the type of LC-forming lipids. The *in vitro* skin permeation study showed that the PABA concentration in skin when applied from the dermis side was higher than when applied from the epidermis side. These findings suggested that oral administration advantageously supports skin targeting, and oral LC formulations could be a promising material in cosmeceutical, dietary and clinical fields.

Keywords: liquid crystals, PABA, oral formulation, bioavailability, skin tissue targeting

1. Introduction:

Skin is utilized as an application site for many topical and transdermal drug delivery systems, and a variety of topical drug formulations have been developed to treat local indications. However, these formulations are not always suitable for treating broad areas of skin, especially in the case of UV protection agents, dietary and cosmetic skin supplements and several skin disorder medicines. Topical application for a broad area skin is often associated with certain drawbacks such as staining of clothes, sweating, pigmentation and skin irritation. Moreover, only a limited number of drugs are amenable to administration by topical application and it is not a practical route to cover large areas of skin on a daily basis [1, 2]. These limitations are associated with a number of drugs not only as medicines for skin disorders but also in dietary and cosmetic skin supplements.

In this study, we aimed to improve the oral bioavailability and skin tissue targeting of *p*-amino benzoic acid (PABA) as a model compound with a formulation approach by utilizing liquid crystals (LCs). LCs are semisolids made of lipids with crystalline structures combining the properties of both crystal and liquid states. Molecules in crystal are highly ordered, while those in liquid are free to diffuse in a random way. Thus, molecules in LC phases diffuse like the molecules in liquid but contain some degree of order [3-6]. A generally used term is the mesophase for LC, indicating such a unique structure is between those of true liquid and solid crystals [7]. In general, LCs can be classified into two categories, *i.e.*, thermotropic and lyotropic. Thermotropic LCs are formed by a change in temperature, whereas lyotropic phases are obtained when mixed with some solvent. Lyotropic LCs usually consist of amphiphilic substances like surfactants and solvents. Amphiphilic substances become micelle at a

low concentration, having cluster of molecules with their polar groups oriented in the water. This is a liquid isotropic phase, where isotropic means identical properties of the structure in all directions. More ordered structures such as hexagonal, lamellar and cubic phases are formed at higher concentrations. These structures are formed, due to insufficient water to fill up spaces between the spherical or elongated micelles [8, 9]. Depending on the solvent concentration and the polarity of solvated mesogen, these systems can undergo phase transitions and structure modifications. Thus, their consistencies and rheological properties can be systematically changed as required [7, 10]. Lyotropic LCs formed with aqueous surfactants can absorb water from the environment, inducing spontaneous phase-transition and forming lamellar phase ($L\alpha$), cubic phase (V_2) and hexagonal phase (H_2) [11, 12]. Among them, cubic phase and hexagonal phase have received much attention due to their highly ordered internal structures, and can be used as a slow release matrix for active pharmaceutical ingredients with various molecular sizes and polarities [13, 14]. Cubic and hexagonal LCs are often spontaneously formed by addition of certain amphiphilic lipids in an aqueous environment [15]. When these LCs are dispersed into nanoparticles by addition of excess water with the stabilizers such as Pluronic copolymers and Myrj series [16], they form stable colloidal dispersions which are termed cubosomes and hexosomes, respectively [17-20].

PABA also known as vitamin Bx was selected as a model compound, which is widely found in foods as a cofactor of the vitamin B complex [21]. PABA is often used as an ingredient in sunscreen owing to its high absorbance in the UVB region, and it is protective against skin cancers. Protection against UV and free radical damage is related to the ability of PABA to scavenge reactive oxygen species [22]. It is also available as a

health supplement (vitamin B₁₀) because of its antioxidant activity [23]. The potassium salt of PABA is used as a prescription drug in the USA for the treatment of skin disorders such as scleroderma, dermatomyositis and Peyronie's disease [24-26]. Based on these findings, PABA is considered as an active element in cosmeceuticals, dietary supplements and skin disorder medicines. However, PABA suffers from a narrow absorption window in the gastrointestinal (GI) tract [27].

During the last few decades, increasing attention has been paid to LC formulations including cubosomes and hexosomes because of their remarkable structural complexity and usefulness in diverse applications [28], but very few studies demonstrated their use *in vivo* or particularly for the investigation of their application in oral drug delivery and skin tissue targeting. The present work was undertaken with the intention of enhancing the oral delivery and skin tissue targeting of PABA using LC formulations and evaluating LCs as a drug delivery system. Oral LC formulations containing PABA were prepared using the following LC forming lipids: glyceryl monooleate (GMO), phytantriol (PHT), C₁₇-monoglycerol ester (MGE) and C₂₂-erythritol ester (ERT) (Fig. 1).

Fig. 1

The confirmation of LC phase structures in the presence of PABA was undertaken by small-angle X-ray scattering (SAXS). The physicochemical measurements of these formulations were performed using a viscometer and a Zetasizer. The *in vitro* release of PABA from LC formulations was determined using a dialysis release method. PABA solution or its dispersed LC formulations were administered to rats, and the pharmacokinetic profile, stomach remaining contents and skin concentration of PABA were determined. Furthermore, the skin permeation and

concentration were investigated using *in vitro* skin permeation studies.

2. Materials and methods

2.1. Materials

PABA was purchased from Kanto Chemical Co., Inc. (Tokyo, Japan). GMO with a normal purity of > 97% and MGE with a normal purity of > 99.56% were purchased from Farnex Co., Inc. (Yokohama, Japan). PHT with a normal purity of > 95% and ERT with a normal purity of > 97% were purchased from Tokyo Chemical Industry Co., Ltd. (Tokyo, Japan). A surfactant, Pluronic[®] F127, was purchased from Sigma-Aldrich (St. Louis, MO, USA). Other reagents and solvents were of special grade or HPLC grade and used without further purification.

2.2. Preparation of PABA-LC formulations

Table 1 shows the composition of dispersed PABA-LC formulations prepared in this study. These formulations were designed based on a 1:1 ratio of the active ingredient (PABA) solution and LC forming lipids. The mixture was dispersed using an ultrasonic homogenizer (USP-50; Shimadzu Corp., Kyoto, Japan) in a pulsing mode (5-s pulse interrupted by 1-s pauses) for 15 min. GMO was melted at 50°C before use, but ERT was hard to melt even at 100°C. Other LC forming lipids were dispersed with PABA solution without preheating. The dispersion for PABA-GMO, -PHT and -MGE formulations produced uniform opaque creamy mixtures. These formulations were able to be orally administered to rats via an oral zonde needle, although a non-uniform mixture with gel-like highly viscous aggregates was observed in case of the PABA-ERT

formulation. No further work was carried out using PABA-ERT formulation owing to high melting point of ERT.

Table 1

2.3. SAXS measurement

SAXS measurement of dispersed PABA-GMO, -PHT and -MGE formulations was performed using a Nano-Viewer (Rigaku, Tokyo, Japan) with a Pilatus 100K/RL 2D detector. The X-ray source was Cu K α radiation with a wavelength of 1.54 Å and operating at 45 kV and 110 mA. The sample-to-detector distance was set at 375 mm. Each sample was placed into a vacuum-resistant glass capillary cell and exposed at 25°C for 10 min. The obtained SAXS pattern was plotted against the scattering vector length, $q = (4\pi/\lambda)\sin(\theta/2)$, where θ is scattering angle. The lattice parameter (a) was obtained from the gradient of the plot of q as a function of $(h^2+k^2+l^2)^{1/2}$ using the following equation: $q = (2\pi/a)\sqrt{h^2 + k^2 + l^2}$, where h , k , and l are the Miller indices. The scattering intensity was normalized by decayed direct beam intensity.

2.4. Measurement of particle size and viscosity

The particle size of LC formulations with or without PABA was measured using a dynamic light scattering Nano-ZS ZEN3600 Zetasizer (Malvern Instruments Ltd., Worcestershire, UK) at 25°C and 37°C. Samples were diluted 10000-fold in water and shaken using a vortex mixer prior to measurement. In addition, the viscosity of LC forming lipids and PABA-LC formulations was measured at 25°C and 37°C using a viscometer (Toki Sangyo Co., Ltd., Tokyo, Japan) that allowed a sensitive determination of viscosity within a range of 0.3-10000 mPa·s with an accuracy of 1% relative error.

2.5. Analytical procedures

The *in vivo* or *in vitro* study sample (50 μ L) was mixed with the same volume of acetonitrile (to precipitate plasma proteins) containing methyl paraben (10 μ g/mL) as an internal standard and centrifuged (5 min, 4°C). The obtained supernatant (20 μ L) was injected into an HPLC system. The HPLC system (Shimadzu, Kyoto, Japan) consisted of a system controller (CBM-20A), pump (LC-20AD), auto-sampler (SIL-20AC), column oven (CTO-20A), a UV detector (SPD-M20A), and analysis software (LC Solution). The column was an Inertsil[®] ODS-3 (5 μ m, 4.6 \times 250 mm) (Nihon Waters K.K.; Tokyo, Japan), which was maintained at 40°C. The mobile phase was acetonitrile : 0.1% phosphoric acid = 8 : 52 (0-4 min), 35 : 65 (4-14 min) and 8 : 92 (14-20 min). The flow rate was adjusted to 1.0 mL/min. PABA was detected at UV 280 nm. In the case of skin samples, the skin piece (0.1 g) was minced with scissors and homogenized (5 min, 4°C) with water (0.9 mL) using a homogenizer (Polytron PT-MR 3000; Kinematica Inc., Littau, Switzerland). The homogenate was mixed with acetonitrile : water = 1:1 (0.5 mL) and agitated for 15 min. After centrifugation (5 min, 4°C), the supernatant (50 μ L) was mixed with the same volume of acetonitrile containing methyl paraben (10 μ g/mL) and centrifuged again (5 min, 4°C). The obtained supernatant (20 μ L) was injected into an HPLC system, and the measurement was obtained with the same conditions as mentioned above.

2.6. *In vitro* dialysis release study

The *in vitro* release study was performed using dialysis bags (Eidia Co., Ltd., Tokyo, Japan). Prior to use, the dialysis bags were soaked in distilled water for 1 h. Phosphate-buffered saline (PBS) as a solvent with physiological pH (7.4) or 0.1 M HCl

to simulate gastric conditions (300 mL each) was used as a receiver medium and continuously stirred at 300 rpm in a beaker and warmed in a water bath at 37°C. A dialysis bag was then loaded with 1 mL of 20 mM PABA or PABA-LC formulation and placed in the beaker. An aliquot (0.5 mL) was withdrawn from the receiver beaker and the same volume of pH 7.4 PBS or 0.1 M HCl was added to the beaker to keep the volume constant. The concentration of released PABA was then determined using an HPLC in conditions as explained in Section 2.5. The cumulative % PABA release was plotted against the square root of time (Higuchi model) [29].

2.7. Animals

Male Wistar rats (200-250 g) were purchased from Sankyo Labo Service Co., Inc. (Hamamatsu, Shizuoka, Japan). Male hairless rats were purchased either from Life Science Research Center, Josai University (Sakado, Saitama, Japan) or Ishikawa Experiment Animal Laboratories (Fukaya, Saitama, Japan). Animals were housed in temperature-controlled rooms ($25 \pm 2^\circ\text{C}$) with a 12 h light-dark cycle (7:00-19:00 h). The rats were allowed free access to food (Oriental Yeast Co., Tokyo, Japan) and tap water. The animal care protocol was approved by the Animal Care and Use Committee of Josai University (Sakado, Saitama, Japan).

2.8. Pharmacokinetic studies and skin samples excising

Intravenous (*i.v.*) and per oral (*p.o.*) administrations were performed in Wistar rats under anesthesia by intraperitoneal (*i.p.*) injection of urethane (1.0 g/kg) to determine the pharmacokinetic parameters of PABA. In case of *i.v.*, PABA dissolved in physiological saline (PABA solution) was injected (10 $\mu\text{mol/kg}$) into the tail vein. Blood samples (0.2 mL) were collected from the jugular vein at predetermined intervals

up to 3 h, and the same volume of saline was injected via the tail vein to prevent severe changes in the volume of distribution. For *p.o.* administration, PABA solution or its dispersed LC-formulation (20 $\mu\text{mol/kg}$) was administered to rats, and blood (0.2 mL) was sampled from the jugular vein at intervals up to 8 h and the same volume of saline was injected via tail vein. Blood samples placed into heparinized tubes were immediately separated by centrifugation to obtain plasma (5 min, 4°C). Skin samples were taken from the abdomen area at 0.5 or 3 h after *p.o.* administration. Plasma and skin samples were stored at -30°C until analysis.

2.9. Determination of PABA concentration remaining in the stomach

Rats were sacrificed at 3 and 8 h after *p.o.* administration of PABA solution or its dispersed LC formulation, and the stomach was removed and the internal lining was scraped with a scalpel blade to collect the stomach contents. The contents were mixed with acetonitrile : ethanol = 2:1 to dissolve the lipid phase and agitated for 15 min. The supernatant (50 μL) after centrifugation (5 min, 4°C) was mixed with the same volume of acetonitrile containing methyl paraben (10 $\mu\text{g/mL}$) and centrifuged (15,000 rpm, 5 min, 4°C) [28]. The obtained supernatant was diluted 100-fold and injected (20 μL) into an HPLC system. The measurement was obtained as described in Section 2.5.

2.10. *In vitro* skin permeation study

Full-thickness hairless rat skin was excised from the abdomen under anesthesia by *i.p.* injection of pentobarbital (50 mg/kg). The excess fat was trimmed off and the skin samples were set in vertical-type diffusion cells (effective diffusion area: 1.77 cm^2) with the epidermis side facing the donor compartment (epidermis to dermis) or facing the receiver compartment (dermis to epidermis). Skin permeation experiments were

conducted after hydration for 60 min with PBS pH 7.4 at 32°C. PABA solution (20 mM, 1.0 mL) and PBS (6.0 mL) were added to the donor and receiver compartments, respectively, in all permeation experiments. The receiver solution was agitated using a stirrer bar and a magnetic stirrer throughout the experiments. An aliquot (0.5 mL) was withdrawn from the receiver chamber and the same volume of PBS was added to keep the volume constant. PABA concentration in the receiver was determined using an HPLC as described in Section 2.5. The donor solution was removed and the skin sample was washed with PBS after the permeation experiment. The permeation area of the skin (1.77 cm²) was then cut and stored at -15°C until analysis. The skin concentration was measured as described in Section 2.5.

2.11. Determination of *AUC*

The area under the plasma concentration-time curve (*AUC*) was calculated using the linear trapezoidal rule. The absolute bioavailability was determined as AUC_{po}/AUC_{iv} , using the mean *AUC* values for *p.o.* and *i.v.* doses. Statistical analysis was performed using unpaired Student's *t*-test (ANOVA), and *P* values less than 0.05 were considered to be significant.

3. Results

3.1. SAXS measurement

The phase behavior of dispersed PABA-LC (PABA-GMO, -PHT and -MGE) formulations was evaluated by SAXS. Figure 2 shows the X-ray diffraction profiles and the lattice parameter (a) of the three PABA-LC formulations. Table 2 summarizes the peak position (q) and intensity of these formulations. These typical reflection patterns; for dispersed PABA-GMO formulation at nearly $\sqrt{2}$, $\sqrt{3}$, $\sqrt{4}$, $\sqrt{6}$, $\sqrt{8}$, $\sqrt{9}$ (a), PABA-PHT formulation at nearly $\sqrt{2}$, $\sqrt{3}$, $\sqrt{4}$, $\sqrt{6}$, $\sqrt{8}$, $\sqrt{9}$ (b) and PABA-MGE formulation at nearly $\sqrt{2}$, $\sqrt{3}$, $\sqrt{4}$, $\sqrt{6}$, $\sqrt{8}$, $\sqrt{9}$ (c), revealed the presence of inverse bicontinuous cubic (V_2) $Pn3m$ phase for the three formulations [30, 31].

Fig. 2 and Table 2

3.2. Measurement of particle size and viscosity

The particle sizes of LC formulations with or without PABA in Pluronic[®] F127 solution was measured by a dynamic light scattering at 25°C and 37°C. Table 3 lists the obtained particle sizes. The particle size was nearly 200-400 nm for all formulations, suggesting that the presence of PABA and temperature changes did not affect the particle size of LC formulations.

Table 3

Moreover, the viscosity of LC forming lipids and their PABA formulations was measured using a viscometer at 25°C and 37°C. Table 4 lists the obtained viscosity values. The viscosity grades of LC forming lipids and their PABA formulations were affected dramatically by changes in experimental temperature, except for the MGE-LC forming lipid and its PABA formulation, suggesting that MGE-LC forming lipid is more thermally stable compared with other LC forming lipids.

Table 4

3.3. *In vitro* dialysis release

The *in vitro* release study was performed using dialysis bags. PBS as a solvent with physiological pH (7.4) or 0.1 M HCl for gastric conditions was used as the receiver medium. Figure 3 shows PABA release profiles from LC formulations into PBS pH 7.4 (a) and 0.1 M HCl (b). The PABA release profile into 0.1 M HCl was similar to that when PBS was used as the receiver medium, indicating that changes in pH probably did not affect the release rate of PABA from its solution or its LC formulations. The PABA release profile from the LC formulations was a relatively slow and gradual till 60 min compared with that from PABA solution. The release profiles of PABA from its GMO and MGE formulations were similar each other. Higuchi's square-root model analysis showed two phases of PABA release; a fast release phase (5-60 min), followed by a slow release phase (60-240 min) of PABA from the LC-matrix. The correlation coefficients of PABA-LC formulations were calculated in accordance with the release profiles obtained using square root Higuchi model as shown in Table 5.

The amount of PABA released from GMO, PHT and MGE were 81 ± 3 , 67 ± 2 and $90 \pm 4\%$, respectively, against the initial dosing. These results showed that the

release profile of PABA from the PHT formulation was slower than that from other PABA-LC formulations and could be related to its high viscosity at 37°C, which could lead to reduced mobility of PABA in this formulation compared with other PABA-LC formulations.

Fig. 3 and Table 5

3.4. Bioavailability of PABA after oral administration

Figure 4 shows the time course of the plasma concentration of PABA after *p.o.* administration of its solution or LC formulations in male Wistar rats. Table 6 summarizes the calculated $AUC_{0-6\text{ h}}$, T_{max} , C_{max} and bioavailability of PABA after administration of PABA solution or its dispersed LC formulations. The C_{max} after oral administration of dispersed PABA-MGE or -GMO formulations was significantly higher than with PABA solution. The T_{max} for administration of dispersed PABA-MGE formulation was faster compared with PABA solution and other PABA-LC formulations. In addition, the bioavailability of PABA was significantly improved by administration of dispersed PABA-MGE or -GMO formulations compared with PABA solution. Although the PABA-PHT formulation resulted in a significant improvement in bioavailability, a relatively lower C_{max} was obtained compared with the other formulations. No plasma concentration was observed 6 h after administration except for the PHT formulation, for which a very low concentration of PABA (3 ± 1 nmol/mL) was observed at 8 h (not shown in Fig. 4).

Fig. 4 and Table 6

3.5. Skin concentration of PABA

Figure 5a and b show the skin concentration of PABA 30 min and 3 h, respectively, after oral administration of PABA solution or its dispersed LC formulation. A significant improvement in the skin concentration at 30 min was observed with the GMO and MGE LC formulations compared with PABA solution, but no improvement was observed using the PHT formulation. No detection of PABA in skin was observed 3 h after application of PABA solution. However, LC formulations sustained a low concentration of PABA in the skin even 3 h after administration. These results suggesting that GMO and MGE formulations were more efficient for enhancing the skin concentration of PABA than PABA solution and PHT formulation.

Fig. 5

3.6. Concentration of PABA remaining in the stomach

In order to estimate the sustained release of PABA from LC formulations, the PABA concentration remaining in the stomach was determined 2 and 8 h after *p.o.* administration of its solution or LC formulation. LC dispersions were observed to accumulate in the pyloric region of the stomach, as shown in Fig. 6. Figure 7 shows nearly 40% of the total dose of PABA concentration from the PHT formulation remained in the stomach 2 h after administration, and nearly 20% remained from the GMO and MGE formulations (Fig. 7a). No PABA was detected 8 h after administration of PABA solution or GMO and PHT formulations, but nearly 12% of the total dose of PABA in the PHT formulation remained in the stomach 8 h after administration (Fig. 7b). The high percentage of PABA remaining in the stomach for the PHT formulation must be consistent with its high viscosity, leading to a prolonged emulsification effect of the formulation in the stomach.

Figs. 6 and 7

3.7. *In vitro* skin permeation study

Figure 8 shows the accumulation time course of PABA that permeated through the skin of full-thickness hairless rat. Almost no change was observed in the skin permeation profile of PABA after application to the epidermis side or the dermis side. However, PABA skin concentration was significantly higher when applied on the dermis side compared with the epidermis-side application, as shown in Fig. 9. This indicated that the partition of PABA to skin tissue from the dermis side was higher than that from the epidermis side; and this supported for usefulness of *p.o.* administration, especially for targeting of PABA to the skin.

Figs. 8 and 9

4. Discussion

The general concept of targeting the skin tissue is by topical application. Very limited studies have emphasized drug-skin tissue targeting via oral administration. The issue to be addressed in this study is that the skin is the largest organ in our body and it is not always suitable to distribute an active ingredient over the whole area of the skin especially for certain indications. Hence, it is necessary to develop oral-skin tissue targeting delivery systems that can effectively deliver a drug to a wide area of skin. Recent studies have shown successful developing of LC formulations that can be applicable for *i.v.* administration [32, 33]. A previous study has demonstrated that PHT dispersions could trigger complement activation, and the process may limit their use for *i.v.* administration as this may initiate infusion-related reactions in sensitive individuals. However, complement activation was significantly milder when PHT was replaced with

GMO [32]. These findings should be considered for the safety concerns of such materials. Minimal studies have been undertaken to investigate potential toxic effects of nanoparticle formulations made from LC forming lipids [34-36]. GMO was reported as a nontoxic, biodegradable and biocompatible material classified as GRAS (generally recognized as safe), and it is included in the FDA *Inactive Ingredients Guide* and in non-parenteral medicines licensed in the UK [37]. Its biodegradability comes from the fact that GMO is subject to lipolysis due to diverse kinds of esterase activity in different tissues [38-40]. In contrast, PHT comprises of a trihydroxy head group and a branched phytanyl tail without the presence of a labile (*e.g.* ester) functionality, which may confer more stability toward enzymatic degradation [41, 42]. A previous study has shown that the *in vitro* toxicity of PHT cubosomes is considerably greater than that of GMO cubosomes. The increased toxicity of PHT appears to result from its greater ability to disrupt the cellular membrane and oxidative stress [42]. No toxicity studies have been reported to investigate the toxic effect of MGE cubosomes. Further efforts are necessary to investigate the potential toxicity of such materials for therapeutic applications.

In this study, we evaluated LC forming lipids formulations as an orally administered drug delivery system for skin tissue targeting. We initially prepared PABA oral formulations using different types of LC forming lipids. The phase behavior of these formulations was determined by SAXS measurement, based on international tables for crystallography [30, 31] obtained reflection patterns for dispersed PABA-GMO formulation at $\sqrt{2}$, $\sqrt{3}$, $\sqrt{4}$, $\sqrt{6}$, $\sqrt{8}$, $\sqrt{9}$ (Fig. 2a), PABA-PHT formulation at $\sqrt{2}$, $\sqrt{3}$, $\sqrt{4}$, $\sqrt{6}$, $\sqrt{8}$, $\sqrt{9}$ (Fig. 2b) and PABA-MGE formulation at $\sqrt{2}$, $\sqrt{3}$, $\sqrt{4}$, $\sqrt{6}$, $\sqrt{8}$, $\sqrt{9}$ (Fig. 2c), thereby confirming the presence of inverse bicontinuous cubic (V_2) $Pn3m$ phase for the prepared formulations (Table 2). These results were consistent with

previous studies on GMO and PHT [43-45]. In addition, the obtained lattice parameters (a) of PABA-GMO formulation (Fig. 2a) and PABA-PHT formulation (Fig. 2b) were consistent with other studies on GMO and PHT [46, 47]. In case of MGE (Fig. 2c), no studies were reported on its formulations phase behavior.

The particle sizes of the LC formulations with or without PABA were measured at 25°C and 37°C. The obtained data showed that the particle size was not affected by changes in temperature or the presence of PABA dispersion (Table 3). Although the particle size of the GMO formulation with or without PABA was smaller compared with other LC formulations, the details were unknown.

The viscosity grade of LC forming lipids and their PABA formulations was dramatically decreased at physiological temperature (37°C) except for MGE and its PABA formulation, which showed almost similar grades at 25°C and 37°C (Table 4). The reason why the viscosity grade of GMO at 25°C was expressed as >10000 mPa.s was due to the viscometer allowing a sensitive determination of viscosity within a range of 0.3-10000 mPa.s. These results suggested that MGE is more thermally stable than GMO and PHT LC forming lipids.

In vitro dialysis release studies showed that there were no changes in the release profiles of PABA in PBS pH 7.4 (Fig. 3a) and in 0.1 M HCl (Fig. 3b), suggesting that changes in the physiological GI tract pH do not affect the release behavior of PABA. The amount of PABA released from its GMO and MGE formulations was 81 ± 3 and $90 \pm 4\%$, respectively, against a dose at 240 min. In case of PABA-PHT formulation, PABA release was slower than that from the PABA solution or other PABA-LC formulations, the amount of PABA released was $67 \pm 2\%$ at 240 min. These results suggested that the high viscosity of PHT at 37°C could affect the drug mobility in its

formulation and its release rate. High correlation coefficients were obtained for each formulation as shown in Table 5, which indicated that *in vitro* drug release profiles of PABA cubosomes were fitted well with the square root Higuchi model. The obtained two phases of PABA release suggested a proposed diffusion mechanism that PABA tends to be adsorbed at the surface of LC during the fast release phase (5-60 min), followed by a slow release phase (60-240 min) of PABA from the LC-matrix. In-depth investigations, the short time taken to achieve more than 50% release of PABA from its LC formulations justifies that these systems are a burst release delivery system where drug is released by diffusion from the cubic phase matrix. Other studies also showed that cubosomes should be classified as a burst release delivery system [8, 48].

In vivo pharmacokinetic studies have shown that the bioavailability of PABA was significantly improved by administration of PABA-LC formulations compared with PABA solution alone (Fig. 4 and Table 6). The C_{max} after oral administration of dispersed PABA-MGE (36 ± 3.7 nmol/mL) or -GMO (27 ± 2.4 nmol/mL) formulation was significantly higher than PABA solution (13 ± 2.3 nmol/mL). The T_{max} after administration of dispersed PABA-MGE (26 ± 9 min) formulation was relatively faster compared with PABA solution (33 ± 5 min) and the PABA-GMO (38 ± 5 min) and -PHT (30 ± 8 min) formulations. In addition, the bioavailability of PABA was significantly improved by administration of dispersed PABA-MGE ($91 \pm 13\%$) or -GMO ($78 \pm 3\%$) formulations compared with PABA solution ($19 \pm 2\%$). Although the PABA-PHT formulation exhibited significantly improved bioavailability ($62 \pm 10\%$), no significant improvement in C_{max} was obtained compared with those for PABA solution and the other formulations. No plasma concentration was observed 6 h after administration except for the PHT formulation, in which a very low concentration of

PABA (3 ± 1 nmol/mL) was observed at 8 h (not showed in Fig. 4). These results suggested that the PABA-MGE formulation was the most efficient formulation for enhancing C_{max} and the bioavailability of PABA. Although the PABA-PHT formulation managed to sustain PABA concentration even at 6 h after administration, the C_{max} was not improved compared with the PABA solution only. In addition, the obtained results suggested that changes in the pharmacokinetic profiles can be observed dependent on the individual LC forming lipid used in the formulation (Fig. 4). Further investigations was done to examine the effect of the physiological temperature, viscosity and the emulsifying effect of the stomach on the pharmacokinetic of PABA. The PABA-PHT formulation showed the highest viscosity at 37°C compared with the other formulations, which was consistent with the high percentage of PABA remaining in the stomach with this formulation compared with the other PABA-LC formulations (Fig. 7). Because the emulsifying ability of the stomach is well known [45], the obtained results suggested that the high viscosity of PHT could delay the emulsifying rate of the PABA formulation in the stomach and consequently could prolong the absorption rate and stomach emptying rate of the dispersed drug. This could be a reason why it managed to sustain the release of PABA for longer hours but with relatively low bioavailability and C_{max} compared with the other formulations.

The other LC forming lipids used in this study was GMO, which is one of the most widely studied LC forming lipids [49]. Our findings showed that the physical state of GMO can be easily affected with the changes in temperature and the viscosity of this LC forming lipid and its PABA formulation was dramatically decreased at 37°C. In addition, the amount of PABA remaining in the stomach using GMO was low compared with the PABA-PHT formulation. These results suggested that this formulation can be

emulsified by the stomach at a faster rate compared with PABA-PHT, and this might offer better drug mobility and influence the movement and absorption of the drug in the intestine. Therefore, it significantly improved bioavailability and C_{max} compared with PABA solution. At the same time, the high viscosity of this LC forming lipid at 25°C makes it not easy to handle, not practical for drug loading and need to melt at 50°C before its use.

In the case of MGE, no studies have utilized this for oral drug delivery. Our finding showed that MGE was more thermally stable compared with other LC forming lipids. The PABA-MGE formulation showed the highest bioavailability and C_{max} and relatively short T_{max} compared with PABA solution and other LC formulations. The low viscosity of MGE at 37°C might offer more drug mobility and drug absorption from the intestine, and this was consistent with the low amount of PABA remaining in the stomach compared with PABA-PHT the formulation (Fig. 7), at the same time its low viscosity at 25°C makes it easy to handle and more practical for drug loading.

In consequence, a non-uniform mixture with gel-like high viscosity aggregates was observed in the preparation of the PABA-ERT formulation, which was related to the high melting point of ERT, making it impractical for designing an oral formulation; therefore, no further work was carried out using this lipid.

Although a significant improvement in skin concentration was observed with the administration of dispersed PABA-GMO or -MGE LC formulations compared with PABA solution at 30 min, no significant enhancement in the skin concentration of PABA was observed using PABA-PHT formulation compared with PABA solution (Fig. 5a). No detection of PABA in the skin was observed 3 h after PABA solution administration. However, dispersed PABA-LC formulations maintained a low

concentration of PABA in the skin even after 3 h (Fig. 5b). As a consequence, as shown in Fig. 4 and Table 6, the C_{max} of PABA after *p.o.* administration of its solution or LC formulations was obtained within 40 min after administration, then the concentration profiles of PABA decreased after 40 min. In addition, the skin concentrations at 30 min were higher than those at 3 h after administration. These results suggested that the skin concentrations of PABA were closely related to its plasma level.

Moreover, *in vitro* skin permeation results showed no changes in the skin permeation profiles of PABA after application of its solution on the epidermis side or on the dermis side (Fig. 8). However, PABA skin concentration was significantly higher after its application on the dermis side compared with its application on the epidermis side (Fig. 9), indicating that the affinity PABA for accumulation in the skin via systemic direction is higher than its delivery via the topical direction; and this could be due to the high barrier function of the stratum corneum. The results obtained in this study advantageously support the concept of targeting PABA to skin.

In conclusion, our obtained data showed that LC formulations are a promising approach to improve the oral absorption and skin tissue targeting of PABA. The PABA-MGE formulation was the most efficient formulation for enhancing C_{max} , bioavailability and skin tissue targeting of PABA compared with other formulations. The pharmacokinetic profiles can be modified based on the type of LC forming lipid used in the formulation design. Despite the changes in the pharmacokinetic profiles that the observed using different LC forming lipids, our main intention was to enhance the oral absorption and skin tissue targeting of PABA and to evaluate LC formulations for oral drug delivery. Further studies need to be conducted to investigate the mechanism of enhancing GI tract-drug absorption using LC formulations. Targeting the skin by orally

dispersed PABA-LC formulations could be a promising achievement in cosmeceutical, dietary and clinical fields.

References

1. Mark RP, Robert L. 2008. Transdermal drug delivery. *Nat. Biotechnol.* 11: 1261-1268.
2. Singh TR, Garland MJ, Cassidy CM, Migalska K, Demir YK, Abdelghany S, Ryan E, Woolfson AD, Donnelly RF. 2010. Microporation techniques for enhanced delivery of therapeutic agents. *Recent Pat Drug Deliv Formul.* 4: 1-17.
3. Spicer PT, Hayden KL. 2001. Novel process for producing cubic liquid crystalline nanoparticles (cubosomes). *Langmuir.* 17: 5748-5756.
4. Yamada K, Yamashita J, Todo H, Miyamoto K, Hashimoto S, Tokudome Y, Hashimoto F, Sugibayashi K. 2011. Preparation and evaluation of liquid-crystal formulations with skin-permeation-enhancing abilities for entrapped drugs. *J Oleo Sci.* 60: 31-40.
5. Schneeweis A, Mueller-Goymann CC. 1997. In vivo and in vitro diclofenac sodium evaluation after rectal application of soft gelatin capsules enabling application induced transformation (AIT) into a semisolid system of liquid crystals (SSLC) for controlled release. *Pharm Res.* 14: 1726-1729.
6. Gin DL, Pecinovsky CS, Bara JE, Kerr L. 2008. Functional lyotropic liquid crystal materials. *Struct Bond.* 128: 181-222.
7. Makai M, Csanyi E, Nemeth Zs, Palinkas J, Eros I. 2003. Structure and drug release of lamellar liquid crystals containing glycerol. *Int J Pharm.* 256: 95-107.
8. Guo C, Wang J, Cao F, Lee RJ, Zhai G. 2010. Lyotropic liquid crystal systems in drug delivery. *Drug Discov Today.* 15: 1032-1040.
9. Siddig MA, Radiman S, Muniandy SV, Jan LS. 2004. Structure of cubic phases in ternary systems gluconone/water/hydrocarbon. *Colloids Surf A Physicochem Eng Asp.* 236: 57-67.
10. Fong WK, Hanley T, Boyd BJ. 2009. Stimuli responsive liquid crystals provide 'on-demand' drug delivery in vitro and in vivo. *J Control Release* 135: 218-226.

11. Clogston J, Rathman J, Tomasko D, Walker H, Caffrey M. 2000. Phase behavior of a monoacylglycerol: (myverol 18-99 K)/water system. *Chem Phys Lipids*. 107: 191-220.
12. Kadhum WR, Todo H, Sugibayashi K. 2015. Skin permeation: Enhancing ability of liquid crystal formulations. In: Dragicevic-Curic N, Maibach H (eds.). *Percutaneous penetration enhancers chemical methods in penetration enhancement: Drug Manipulation Strategies and Vehicle Effects*. Springer-Verlag Berlin Heidelberg. pp. 243-253.
13. Drummond CJ, Fong C. 1999. Surfactant self-assembly objects as novel drug delivery vehicles. *Curr Opin Colloid Interface Sci*. 4: 449-456.
14. Shah JC, Sadhale Y, Chilukuri DM. 2001. Cubic phase gels as drug delivery systems. *Advanced Drug Delivery Reviews*. 47: 229-250.
15. Kaasgaard T, Drummond CJ. 2006. Ordered 2-D and 3-D nanostructured amphiphile self-assembly materials stable in excess solvent. *Phys Chem Chem Phys*. 8: 4957-4975.
16. Chong JYT, Mulet X, Waddington LJ, Boyd BJ, Drummond CJ. 2012. High-throughput discovery of novel steric stabilizers for cubic lyotropic liquid crystal nanoparticle dispersions. *Langmuir*. 28: 9223-9232.
17. Spicer PT. 2005. Progress in liquid crystalline dispersions: cubosomes. *Curr Opin Colloid Interface Sci*. 10: 274-279.
18. Yaghmur A, Glatter O. 2009. Characterization and potential applications of nanostructured aqueous dispersions. *Adv Colloid Interface Sci*. 148: 333-342.
19. Lancelot A, Sierra T, Serrano JL. 2014. Nanostructured liquidcrystalline particles for drug delivery. *Expert Opin Drug Deliv*. 11: 1-18.
20. Hirlekar R, Jain S, Patel M, Garse H, Kadam V. 2010. Hexosomes: a novel drug delivery system. *Curr Drug Deliv*. 7: 28-35.
21. Sonja S, Nikola G, Robert Z, Wolfgang S. 2010. Oxidation of ortho- and para-amino benzoic acid. A pulse radiolysis-and gamma radiolysis study. *Radiat Phys Chem*. 80: 932-936.

22. Hu ML, Chen YK, Chen LC, Sano M. 1995. Para-aminobenzoic acid scavenges reactive oxygen species and protects DNA against UV and free radical damage. *J Nutr Biochem.* 6: 504-508.
23. Akberova SI. 2002. New biological properties of p-aminobenzoic acid. *Biology Bulletin.* 29: 390-393.
24. Rashmi SS, Raechel CJ, Carol JB, Mario GF, Alexei PL, Megan AM. 2013. Effects of Para-Aminobenzoic Acid (PABA) form and administration mode on PABA recovery in 24-Hour Urine Collections. *J Acad Nutr Diet.* 114: 458-463.
25. Zarafonetis CJ, Dabich L, Skovronski JJ. 1988. Retrospective studies in scleroderma: skin response to potassium para-aminobenzoate therapy. *Clin Exp Rheumatol.* 6: 261-268.
26. Zarafonetis CJ, Dabich L, Negri D. 1988. Retrospective studies in scleroderma: effect of potassium para-aminobenzoate on survival. *J Clin Epidemiol.* 41: 193-205.
27. Ichikawa M, Watanabe S, Miyake Y. 1991. A new multiple-unit oral floating dosage system. II: In vivo evaluation of floating and sustained release characteristics with para amino benzoic acid and iso sorbide di nitrate as model drugs. *J Pharm Sci.* 80: 1153-1156.
28. Nguyen TH, Hanley T, Porter CJ, Boyd BJ. 2011. Nanostructured liquid crystalline particles provide long duration sustained-release effect for a poorly water soluble drug after oral administration. *J Control Release.* 153: 180-186.
29. Higuchi T. 1963. Mechanism of sustained action medication: theoretical analysis of rate of release of solid drugs dispersed in solid matrices. *J Pharm Sci.* 52: 1145-1148.
30. Anderson DM, Gruner SM, Leibler S. 1988. Geometrical aspects of the frustration in the cubic phases of lyotropic liquid crystals. *Proc Natl Acad Sci USA.* 85: 5364-5368.
31. Qiu H, Caffrey M. 2000. The phase diagram of monoolein/water system: metastability and equilibrium aspects. *Biomaterials.* 21: 223-234.
32. Azmi ID, Wu L, Wibroe PP, Nilsson C, Østergaard J, Stürup S, Gammelgaard B, Urtti A, Moghimi SM, Yaghmur A. 2015. Modulatory effect of human plasma on

the internal nanostructure and size characteristics of liquid-crystalline nanocarriers. *Langmuir*. 31: 5042-5049.

33. Wibroe PP, Azmi ID, Nilsson C, Yagmur A, Moghimi SM. 2015. Citrem modulates internal nanostructure of glyceryl monooleate dispersions and bypasses complement activation: Towards development of safe tunable intravenous lipid nanocarriers. *Nanomedicine*. 11: 1909-1914.
34. Barauskas J, Cervin C, Jankunec M, Spandyreva M, Ribokaite K, Tiberg F, Johnsson M. 2010. Interactions of lipid-based liquid crystalline nanoparticles with model and cell membranes. *Int J Pharm*. 391: 284-291.
35. Murgia S, Falchi AM, Mano M, Lampis S, Angius R, Carnerup AM, Schmidt J, Diaz G, Giacca M, Talmon Y, Monduzzi M. 2010. Nanoparticles from lipid-based liquid crystals: emulsifier influence on morphology and cytotoxicity. *J Phys Chem*. 114: 3518-3521.
36. Shen HH, Crowston JG., Huber F, Saubern S., McLean KM. and Hartley PG. 2010. The influence of dipalmitoyl phosphatidylserine on phase behaviour of and cellular response to lyotropic liquid crystalline dispersions. *Biomaterials*. 31: 9473-9481.
37. Ganem-Quintanar A, Quintanar-Guerrero D, Buri P. 2000. Monoolein: a review of the pharmaceutical applications. *Drug Dev Ind Pharm*. 26: 809-820.
38. Ericsson B, Ericsson PO, Lofroth JE, Engstrom S. 1991. Cubic phases as delivery systems for peptide drugs. *Am Chem Soc Symp Ser*. 469: 251-265.
39. Boyle E, German JB. 1996. Monoglycerides in membrane systems. *Crit Rev Food Sci Nutr*. 36: 785-805.
40. Longer M, Tyle P, Mauger JW. 1996. A cubic-phase oral drug delivery system for controlled release of AG337. *Drug Dev Ind Pharm*. 22: 603-608.
41. Shen HH, Crowston JG, Huber F, Saubern S, McLean KM, Hartley PG. 2010. The Influence of Dipalmitoyl Phosphatidylserine on Phase behaviour of and Cellular response to Lyotropic Liquid Crystalline Dispersions. *Biomaterials*. 31: 9473-9481.

42. Hinton TM, Grusche F, Acharya D, Shukla R, Bansal V, Waddington LJ, Monaghan P, Muir BW. 2014. Bicontinuous Cubic Phase Nanoparticle Lipid Chemistry Affects Toxicity in Cultured Cells. *J Toxicol Res.* 3: 11-22.
43. Barauskas J, Landh T. 2003. Phase behaviour of the phytantriol/water system. *Langmuir.* 19: 9562-9565.
44. Briggs J, Chung H, Caffrey M. 1996. The temperature-composition phase diagram and mesophase structure characterization of the monoolein/water system. *J Phys II France.* 6: 723-751.
45. Kathy WYL, Nguyen TH, Hanley T, Boyd BJ. 2009. Nanostructure of liquid crystalline matrix determines in vitro sustained release and in vivo oral absorption kinetics for hydrophilic model drugs. *Int J Pharm.* 365: 190-199.
46. Bu M, Tang J, Wei Y, Sun Y, Wang X, Wu L, Liu H. 2015. Enhanced bioavailability of nerve growth factor with phytantriol lipid-based crystalline nanoparticles in cochlea. *Int J Nanomedicine.* 10:6879-6889.
47. Yaghmur A, Rappolt M, Østergaard J, Larsen C, Larsen SW. 2012. Characterization of bupivacaine-loaded formulations based on liquid crystalline phases and microemulsions: the effect of lipid composition. *Langmuir.* 28: 2881-2889.
48. Boyd BJ. 2003. Characterisation of drug release from cubosomes using the pressure ultrafiltration method. *Int J Pharm.* 260: 239-47.
49. Larsson K. 1999. Colloidal dispersions of ordered lipid-water phases. *J Dispersion Sci Technol.* 20: 27-34.

Tables

Table 1

Composition of dispersed PABA-LC formulations

Ingredients (%)	PABA-GMO 20 mM	PABA-PHT 20 mM	PABA-MGE 20 mM	PABA-ERT 20 mM
GMO	30	---	---	---
PHT	---	30	---	---
MGE	---	---	30	---
ERT	---	---	---	30
PABA solution	30	30	30	30
Purified water containing 5% Pluronic® F127	40	40	40	40
Total %	100	100	100	100

Abbreviations: PABA, *p*-amino benzoic acid; LC, liquid crystal; GMO, glyceryl monooleate; PHT, phytantriol; MGE, C₁₇-monoglycerol ester; ERT, C₂₂-erythritol ester.

Table 2

Peak position (q) and intensity observed in Bragg reflection of PABA-LC formulations

Formulation	Peak position (q) (nm^{-1})	Intensity (cps)
PABA-GMO	0.982	1412
	1.203	545.8
	1.388	219.8
	1.623	192
	1.979	169
PABA-PHT	1.352	698
	1.659	470
	1.915	169
	2.376	126
	2.772	64
PABA-MGE	1.381	1088
	1.694	609
	1.95	189
	2.406	136
	2.755	69

Abbreviations: the same in Table 1.

Table 3

Particle size (nm) of LCs

	Dispersed with PABA at 25°C	Dispersed with PABA at 37°C	Without PABA at 25°C	Without PABA at 37°C
GMO	212 ± 15	254 ± 12	244 ± 21	239 ± 23
PHT	332 ± 31	361 ± 34	319 ± 22	352 ± 38
MGE	289 ± 25	320 ± 31	311 ± 27	306 ± 12

Abbreviations: the same in Table 1.

Each value represents the mean ± S.E. of 3 experiments.

Table 4

Rheological properties of LC forming lipids and LC formulations

	At 25°C	At 37°C
GMO alone*	> 10000	187 ± 23
PHT alone*	8619 ± 34	2019 ± 103
MGE alone*	560 ± 41	175 ± 27
PABA-GMO formulation	6422 ± 133	2193 ± 213
PABA-PHT formulation	7231 ± 183	4331 ± 198
PABA-MGE formulation	1890 ± 201	1101 ± 112

Abbreviations: the same in Table 1.

*: LC forming lipid only without water or any additive.

Each viscosity (mPa.s) represents the mean ± S.E. of 3 experiments.

Table 5

Correlation coefficients* of PABA-LC formulations

	Fast release phase (pH 7.4)	Slow release phase (pH 7.4)	Fast release phase (0.1 M HCl)	Slow release phase (0.1 M HCl)
PABA-GMO	0.9965	0.9993	0.9965	0.9992
PABA-PHT	0.9902	0.9974	0.9937	0.9904
PABA-MGE	0.9936	0.9973	0.9881	0.9791

Abbreviations: the same in Table 1.

*: The correlation coefficients were obtained by data from 5-60 and 60-240 min as a represent to the fast release phase and the slow release phase, respectively.

Table 6

Pharmacokinetic parameters of PABA after oral administration of its solution or its dispersed LC formulation

	AUC_{0-6h}	T_{max} (min)	C_{max} (μ M)	Bioavailability $_{0-6h}$ (%)
PABA solution	774 ± 77	33 ± 5	13 ± 2.3	19 ± 2
GMO-PABA	$3203 \pm 107^*$	38 ± 5	$27 \pm 2.4^*$	$78 \pm 3^*$
PHT-PABA	$1467 \pm 98^*$	30 ± 8	15 ± 0.89	$62 \pm 10^*$
MGE-PABA	$3887 \pm 539^*$	26 ± 9	$36 \pm 3.7^*$	$91 \pm 13^*$

Abbreviations: the same in Table 1.

Each value shows the mean \pm S.E. of 3 experiments.*: $P < 0.05$ significantly different from PABA solution (Student's t -test).

Figure captions

Fig. 1. Chemical structures of glyceryl monooleate (GMO), phytantriol (PHT), C₁₇-monoglycerol ester (MGE) and C₂₂-erythritol ester (ERT).

Fig. 2. Small-angle X-ray scattering (SAXS) profiles and lattice parameter (*a*) of *p*-amino benzoic acid (PABA)-glyceryl monooleate (GMO) formulation (a), PABA-phytantriol (PHT) formulation (b) and PABA-C₁₇-monoglycerol ester (MGE) formulation (c).

Fig. 3. Percentage of *p*-amino benzoic acid (PABA) release profiles into phosphate-buffered saline (PBS) pH 7.4 (a) and 0.1 M HCl (b). Symbols: (●), PABA solution; (○), PABA-glyceryl monooleate (GMO) formulation; (△), PABA-phytantriol (PHT) formulation; and (□) PABA-C₁₇-monoglycerol ester (MGE) formulation. Dashed line showing two release phases of PABA from its LC formulations. Each point represents the mean ± S.E. of three experiments.

Fig. 4. Plasma profiles of *p*-amino benzoic acid (PABA) after oral administration. Symbols: (●), PABA-glyceryl monooleate (GMO) formulation; (○), PABA-GMO formulation; (△), PABA-phytantriol (PHT) formulation; and (□) PABA-C₁₇-monoglycerol ester (MGE) formulation. Each point represents the mean ± S.E. of three experiments.

Fig. 5. Skin concentration of *p*-amino benzoic acid (PABA): (a) 30 min after oral administration of PABA solution or its liquid crystal (LC) formulation; (b) 3 h after oral administration of PABA solution or its LC formulation. Each column represents the mean ± S.E. of three experiments. *: $P < 0.05$ significantly different from PABA solution (Student's *t*-test).

Fig. 6. An illustrative photograph of the remaining dispersed *p*-amino benzoic acid (PABA)-liquid crystal (PABA-LC) formulation in the stomach of rats after oral administration.

Fig. 7. The percentage of *p*-amino benzoic acid (PABA) remaining in the stomach: (a) 2 h after oral administration of PABA solution or its dispersed liquid crystal (LC) formulation; (b) 8 h after oral administration of PABA solution or its dispersed LC formulation. Each column represents the mean \pm S.E. of three experiments.

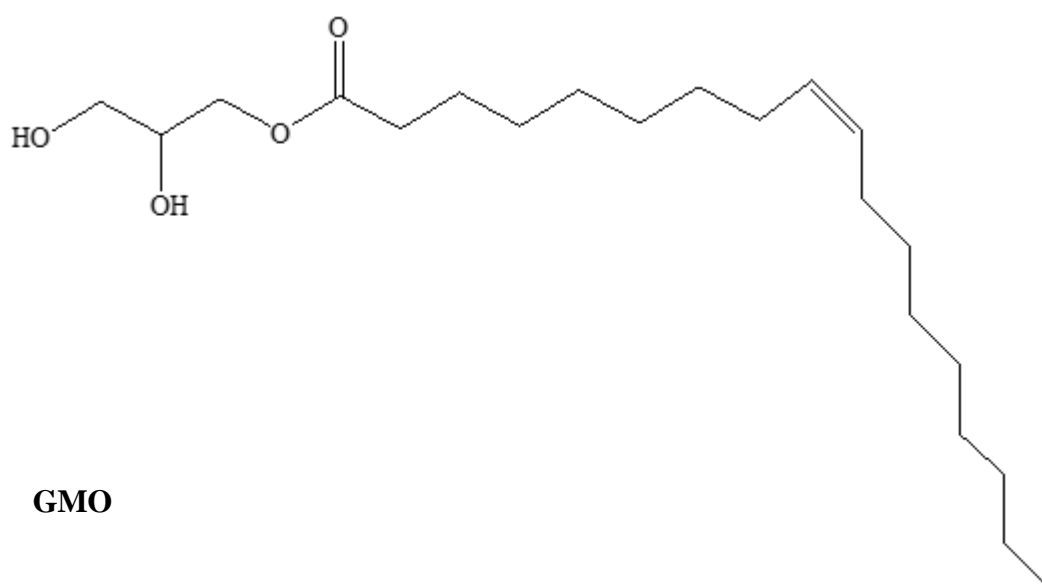
Fig. 8. *In vitro* skin permeation study: time course of the cumulative amount of *p*-amino benzoic acid (PABA) that permeated through full-thickness hairless rat skin. Symbols: (■), from the dermis to epidermis; and (Δ), from the epidermis to dermis. Each point shows the mean \pm S.E. of three experiments.

Fig. 9. Skin concentration of *p*-amino benzoic acid (PABA) after an 8 h *in vitro* skin permeation experiment. Each column represents the mean \pm S.E. of three experiments.

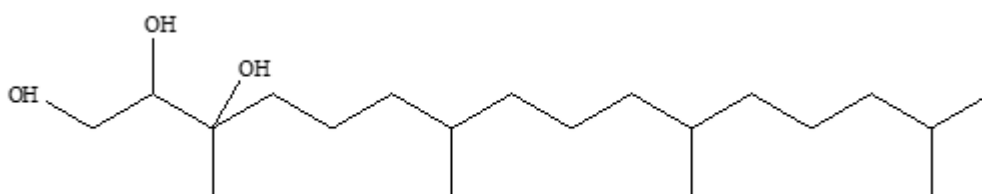
*: $P < 0.05$ significantly different from the epidermis to dermis (Student's *t*-test).

Figures

Fig. 1



GMO



PHT

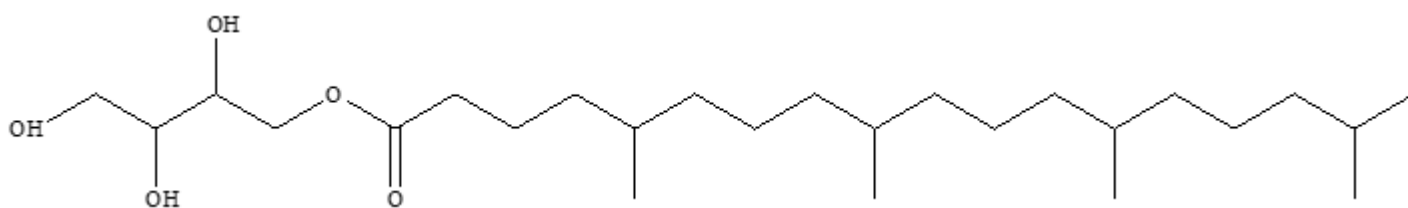
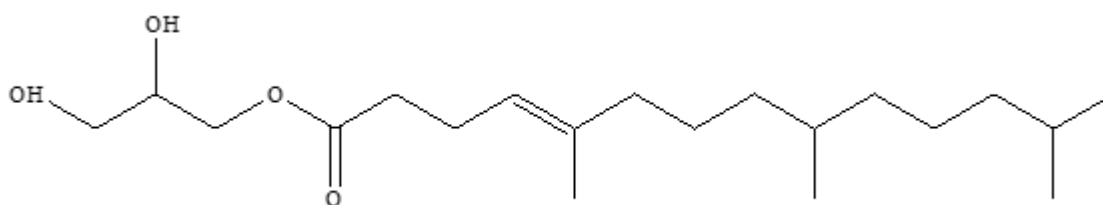
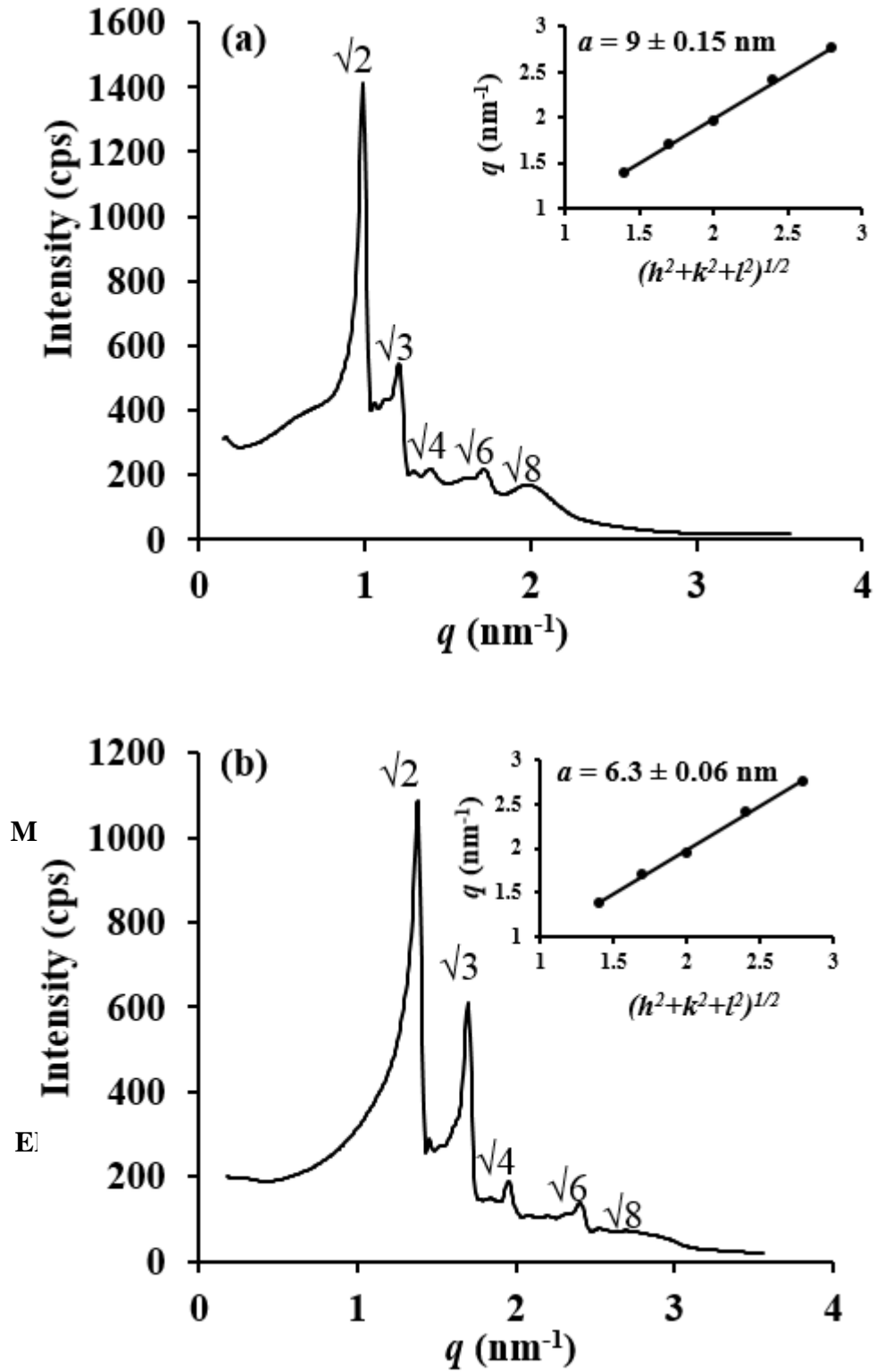


Fig. 2



Continue to Fig. 2

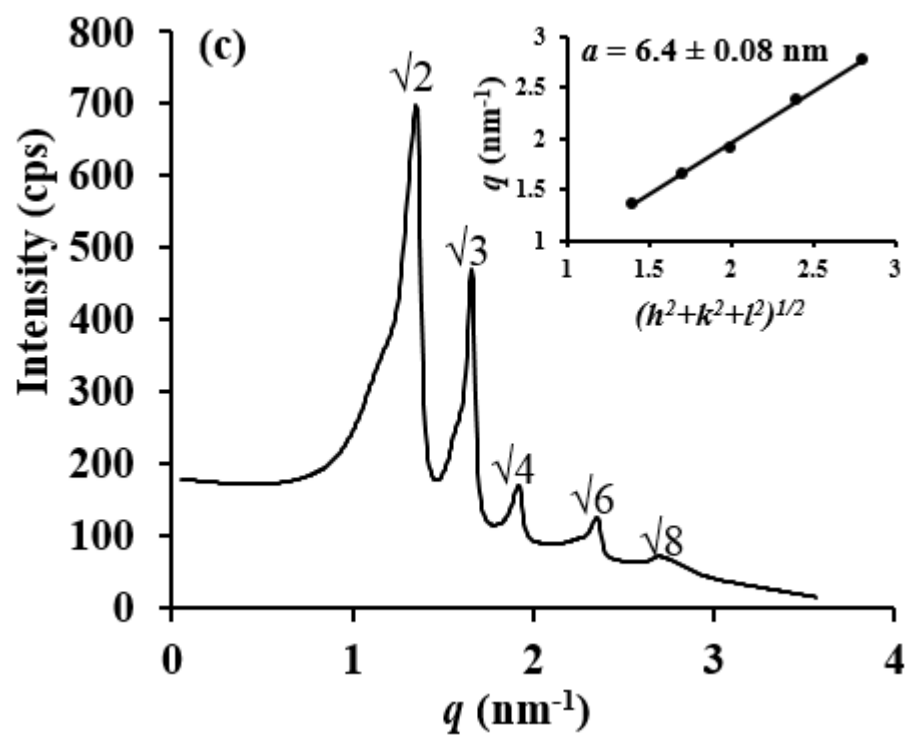


Fig. 3

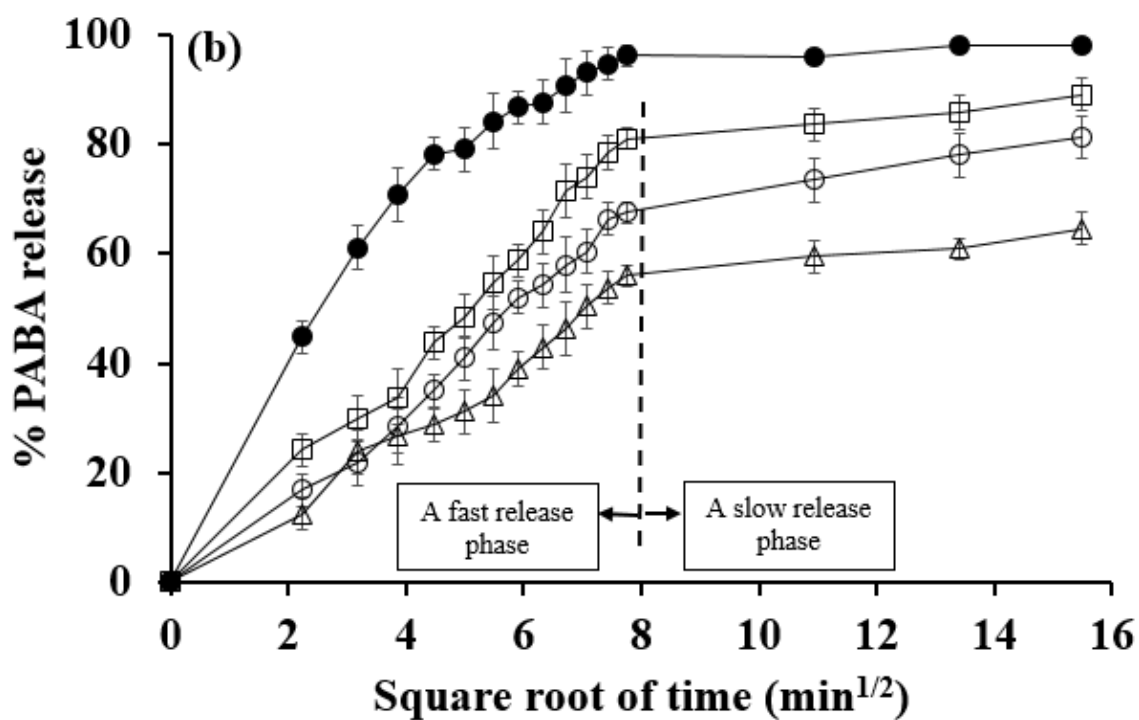
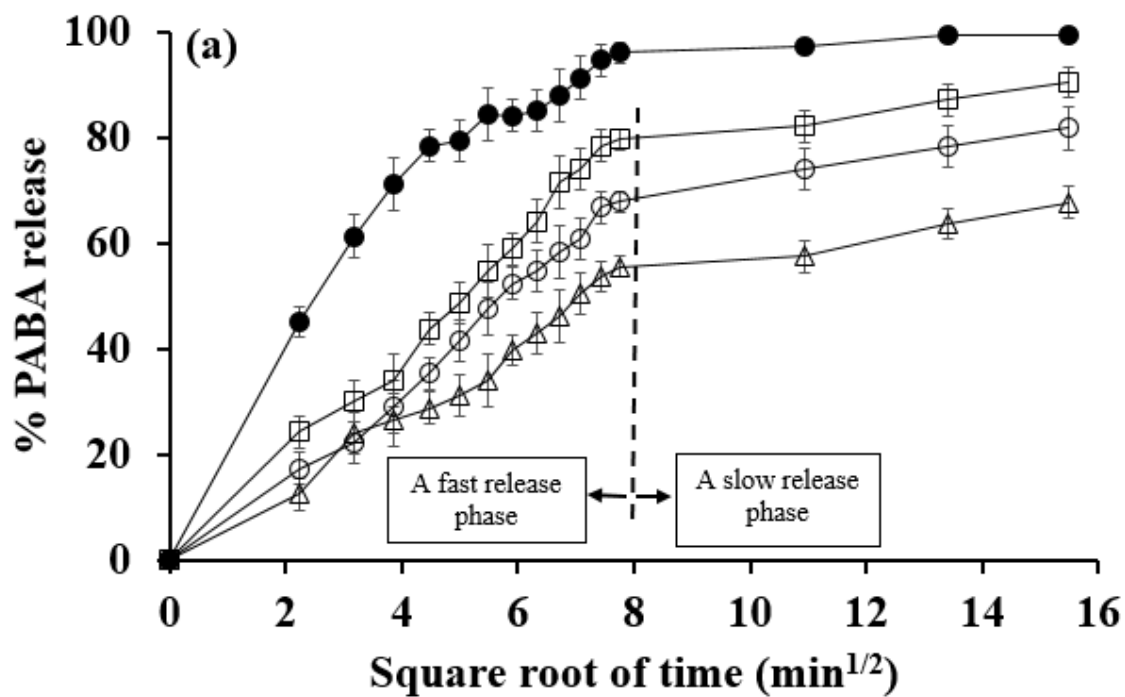


Fig. 4

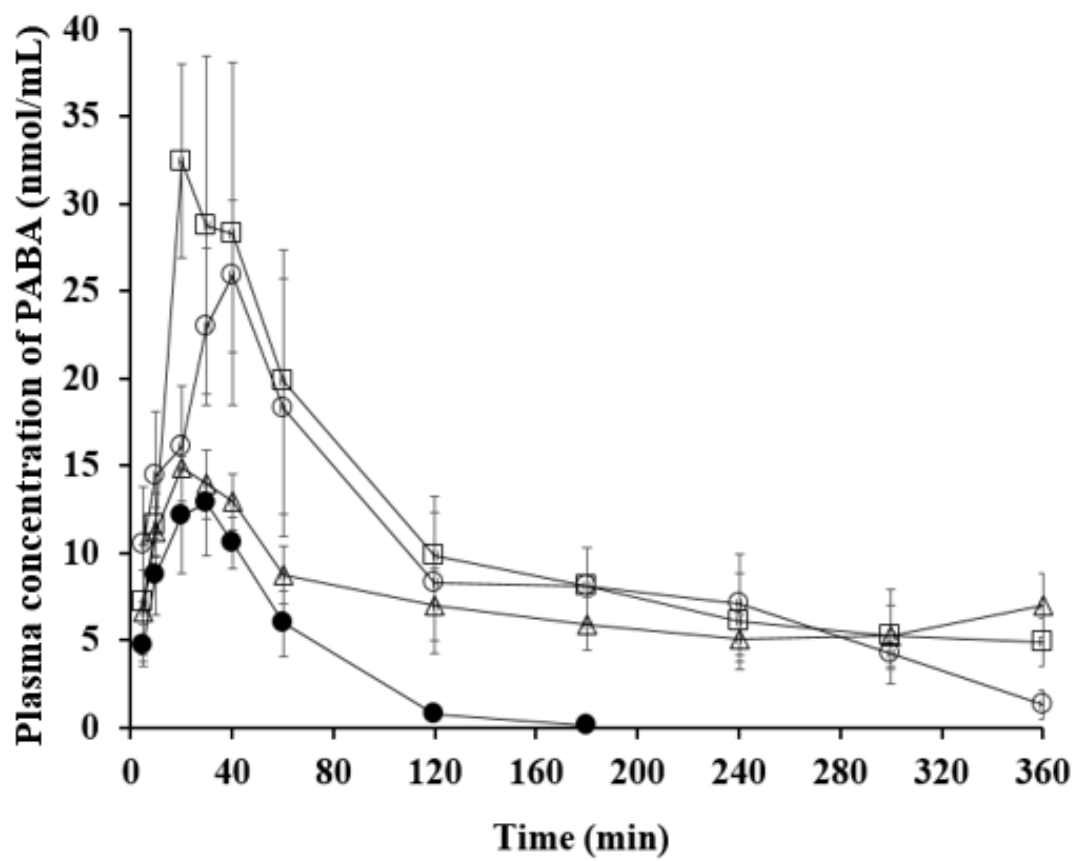


Fig. 5

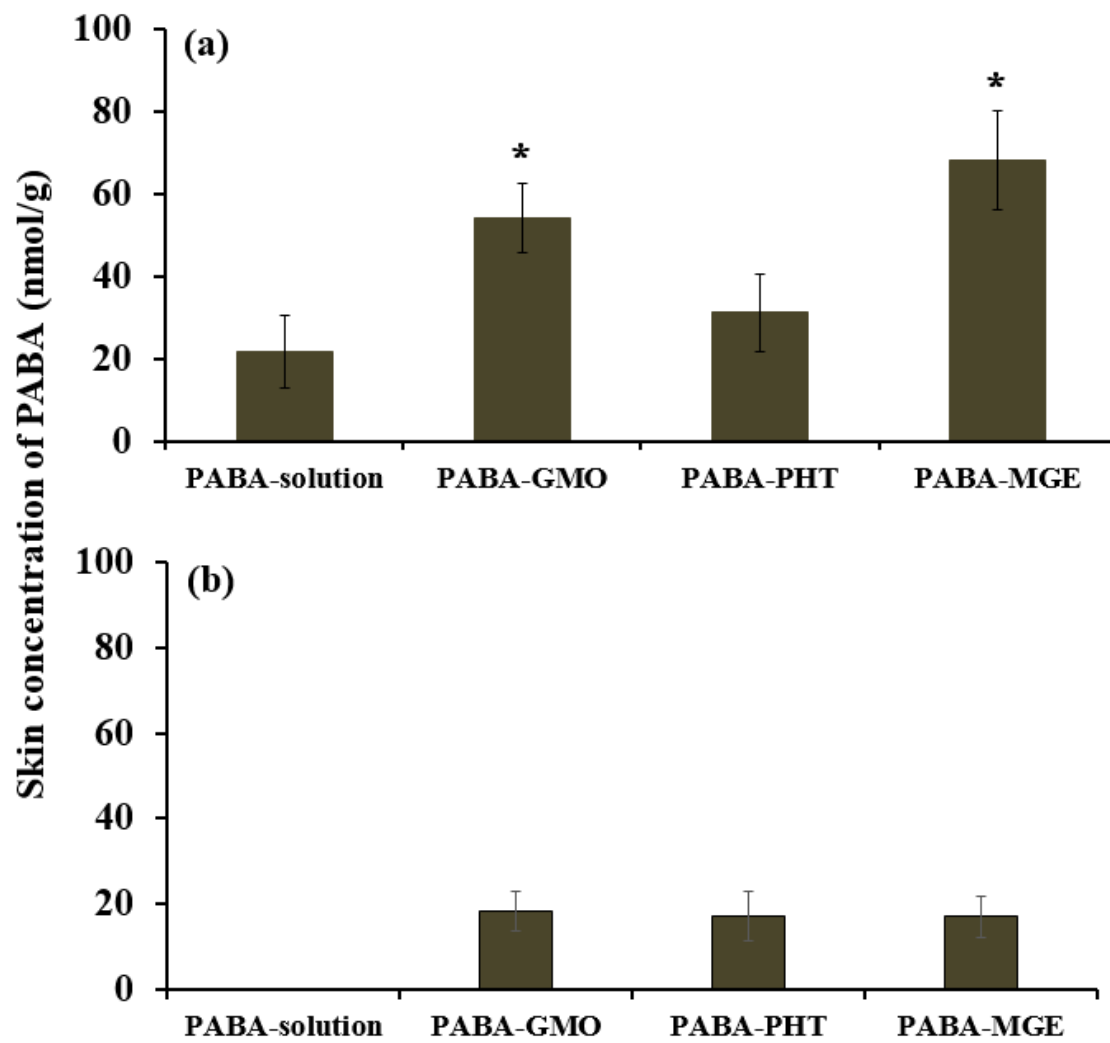


Fig. 6

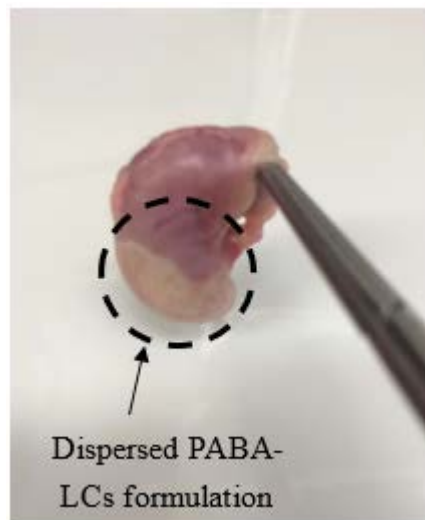


Fig. 7

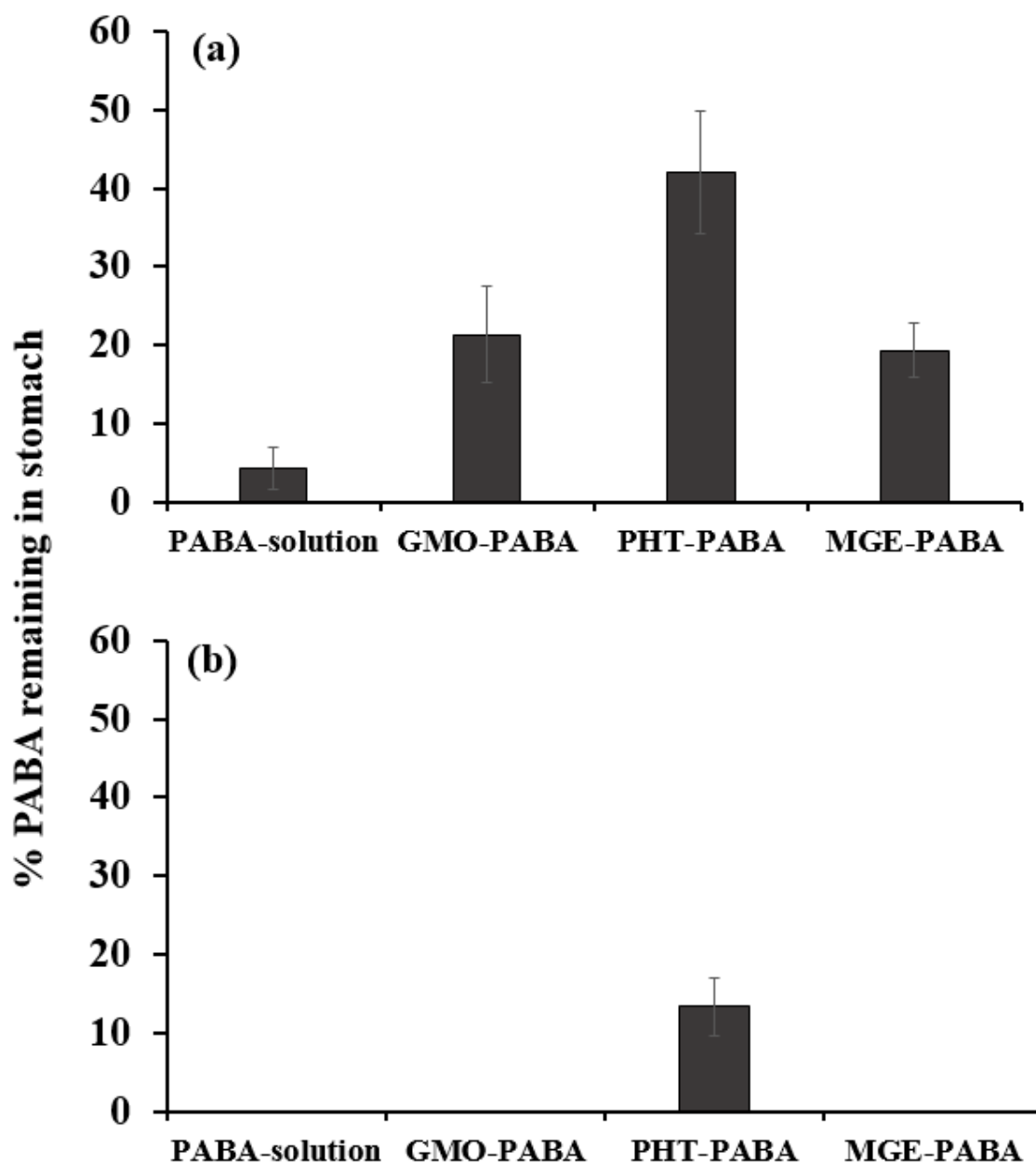


Fig. 8

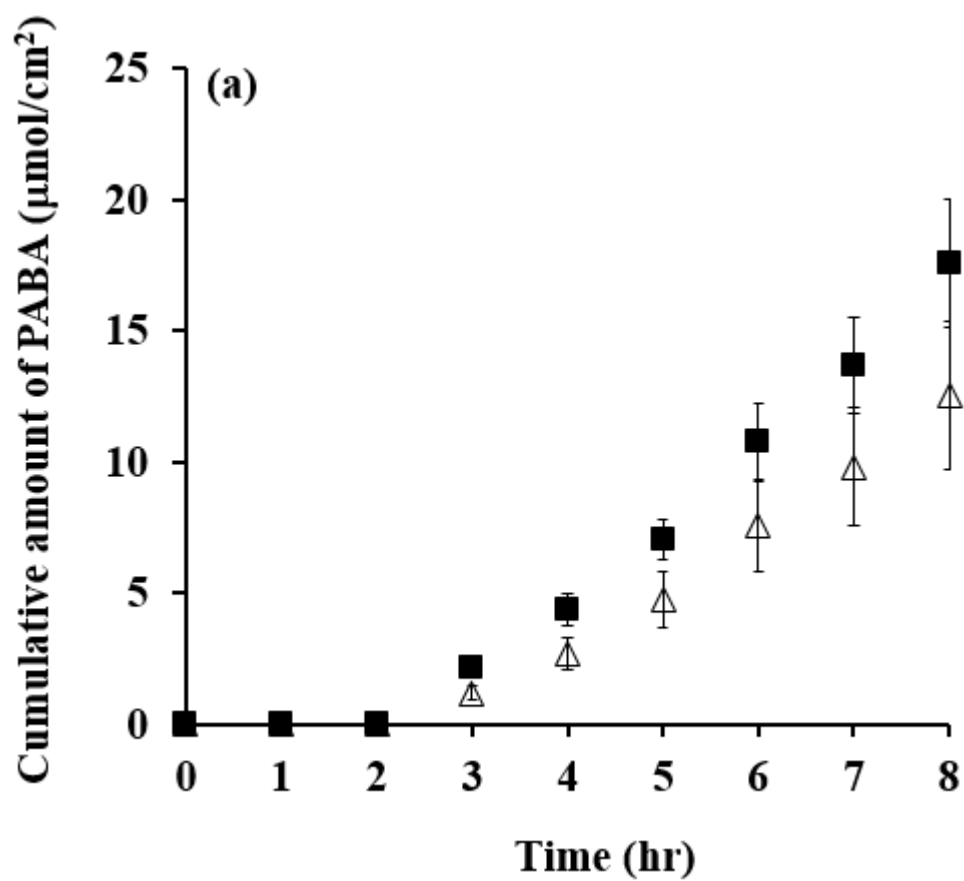


Fig. 9

